Progress In Electromagnetics Research Letters, Vol. 110, 101–108, 2023

Ultracompact Mode-Division (de)Multiplexer Based on Lithium Niobate Waveguide

Hua Liu[1], Fang Wang[1, 3, *], Tao Ma[4], Shoudao Ma[1], and Yufang Liu[2]

Abstract—We present an ultra-compact modular division (de)multiplexer [(de)MUX] based on the lithium niobate waveguide, an asymmetric directional coupler (ADC) composed of silica-lithium niobate waveguide (SLNW) and lithium niobate waveguide (LNW) for the modular division multiplexer. The TE0 and TE1 modes were optimized by using the finite element method (FEM). By rationally designing the size of SLNW and LNW, TE0 mode light is injected into the In1 port of LNW, and TE0 mode light is converted to TE1 mode in the coupling zone and transmitted in the SLNW, output from the Out2 port. It is shown that the coupling length of this MUX is only 6 μm. At a working wavelength of 1.55 μm, when TE0 enters the coupling area from port In1, the mode is coupled and converted to TE1; the TE1 mode is output from Out2; the value of IL is 0.87 dB; and the value of MCE is 99.5%. When TE0 enters from port In2, the TE0 mode is output from Out2, with 0.1 dB for IL, 99.7% for MCE, and −25 dB for CT.

1. INTRODUCTION

In order to meet the high bandwidth demand of massively parallel chip multi-processors, on-chip optical interconnection with ultra-high transmission capacity is urgently needed [1, 2]. Mode-division multiplexing (MDM) is one of the most promising methods for enhancing the capacity of optical communication systems. The mode (de)multiplexer [(de)MUX] plays a key role in the MDM system by converting several single patterns in different input channels to the higher-order patterns required in the main channel and vice versa [3, 4].

Mode division multiplexing technology is a kind of spatial multiplexing technology, which uses different modes in fiber or waveguide as different transmission channels to realize data transmission [5]. To achieve high-performance mode multiplexer MUX, several approaches have been reported, such as asymmetric directional couplers (ADC), adiabatic couplers (AC), multimode interference (MMI) waveguides, microloops, and asymmetric Y structures [6–10]. Mode MUX with broadband width and loose manufacturing tolerance can be realized based on mode evolution AC [11]; however, mode MUX based on AC occupies a relatively large space. Another approach uses mode MUX based on MMI waveguides, which can provide broadband width and large manufacturing tolerances [12]. However, mode MUX based on MMI waveguides always requires phase shifters, which are very sensitive to manufacturing errors. Chen et al. reported a three-mode MUX based on two cascading Y branches [13], in which a high extinction ratio (ER) of 31.5 dB could be achieved. However, the structure is relatively long and requires rigorous manufacturing because of the tiny gap between the two branches. ADC-based mode MUX is very compact and can be freely cascaded to reuse more modes [14].

Received 14 February 2023, Accepted 23 April 2023, Scheduled 11 May 2023

* Corresponding author: Fang Wang (021034@htu.edu.cn).

[1] College of Electronic and Electrical Engineering, Henan Normal University, Xinxiang 453007, China. [2] Henan Key Laboratory of Optoelectronic Sensing Integrated Application, Xinxiang 453007, China. [3] Academician Workstation of Electromagnetic Wave Engineering of Henan Province, Xinxiang 453007, China. [4] Henan Engineering Laboratory of Additive Intelligent Manufacturing, Xinxiang 453007, China.

Optical mode sizes in lithium-niobate-on-insulator (LNOI) waveguides are typically reduced by more than an order of magnitude compared to their high-capacity counter components [15], which is beneficial for compact photonic devices. LNOI is an excellent platform for integrating photonic devices because of its outstanding features, such as a wide transparency range from 350 nm to 5200 nm and strong electro-optic, acoustooptic, and thermos-optic effects. Lithium niobate is a mature electro-optic material with stable physical and chemical properties, high electro-optical coefficient and low optical absorption loss. It is an ideal platform for photonic integrated circuits (PIC). Thin film lithium niobate (LN) overcomes the large size limitations of conventional titanium diffusion and proton exchange LN.

In this paper, an ultra-compact mode-division (de)multiplexer [(de)MUX] based on a lithium niobate waveguide is proposed. The design principle of MUX is discussed, and the geometric parameters of the structure are optimized at 1.55 μm wavelength, while discussing the performance of MUX. We proposed that MUX can drive several important optical functions, from free space to the chip. The structure of the article is arranged as follows. The second part is the design of the MUX waveguide structure. The third part is the modal properties of the MUX structure parameters. In the fourth part, the Mode division multiplexing properties of MUX are discussed and analyzed. The fifth part is the manufacturing process.

2. WAVEGUIDE STRUCTURE

The proposed structure of the Mode division multiplexer based on the asymmetrically oriented directional coupler is shown in Fig. 1. Fig. 1(a) shows that the asymmetrically oriented coupler consists of SLNW and LNW. The SLNW consists of a niobate waveguide and SiO_2 strip waveguide. The cross section of the Mode division multiplexer is shown in Fig. 1(b). The structural parameter definition and some default parameters of the device are set as follows. The thickness of the lithium niobate waveguide in the device is $H_1 = 500$ nm, and the height of the SiO_2 waveguide in the SLNW is $H_{SiO_2} = 210$ nm. The width of the LNW is W_1; the width of the SLNW is W_2; the spacing between the SLNW and LNW waveguides is G, and the coupling length is L_1. The device mainly consists of the SLNW and LNW, where the input ports are In1 and In2, and the output waveguide ports are Out1 and Out2. In this design, at an operating wavelength of 1.55 μm, the refractive index of LN is $ne = 2.1381$, $no = 2.2112$, and the refractive index of SiO_2 is $nSiO_2 = 1.44$.

The working mode of the multiplexer is TE mode, specifically TE0 and TE1 mode. The working principle of the Mode division multiplexer can be described as follows, and the size of the waveguide is reasonably optimized, so that the TE base mode (namely TE0) in the LNW in the coupling area is close to the effective refractive index of the TE1 mode in the SLNW, which meets the phase matching condition. Under this condition, the TE0 mode from the input port In1 can be fully coupled to the

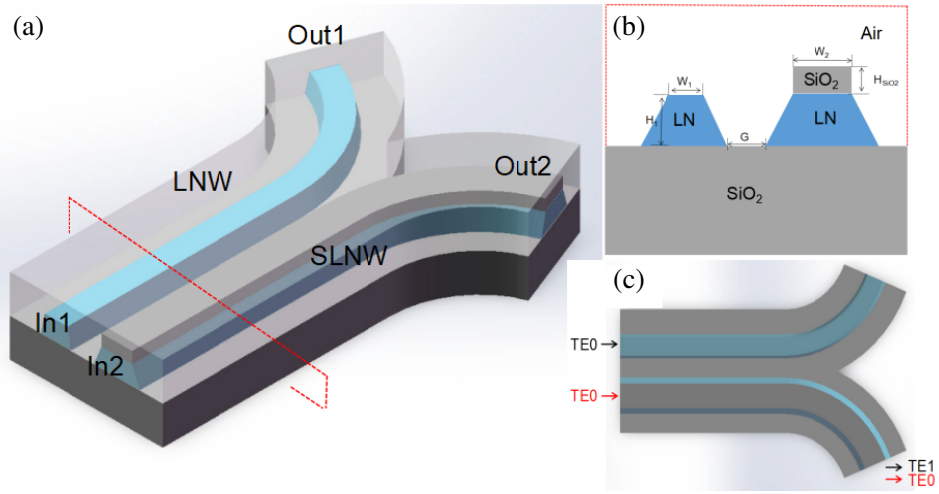

Figure 1. Mode multiplexer, (a) 3D view, (b) cross section and (c) top view.

SLNW after transmitting a specific distance within the coupling area and converted into a stable TE1 mode in the waveguide and finally output from the SLNW output port Out2. The TE0 mode input from another input port In2 transmits forward along the SLNW, and almost no coupling occurs in the coupling area and finally output from Out2. Finally, we can detect both TE0 and TE1 modes at the output port Out2, realizing the function of Mode division multiplexing.

To evaluate the performance of the mode division multiplexers, the mode conversion efficiency (MCE), crosstalk (CT), and insertion loss (IL) are usually used.

$$\mathrm{MCE} = \frac{P_{\mathrm{Out2}}}{P_{\mathrm{Out1}} + P_{\mathrm{Out2}}} \tag{1}$$

$$\mathrm{CT\,(dB)} = 10\log_{10}\frac{P_{\mathrm{Out2}}}{P_{\mathrm{Out1}}} \tag{2}$$

$$\mathrm{IL\,(dB)} = -10\log_{10}\frac{P_{\mathrm{Out2}}}{P_{\mathrm{In1}}} \tag{3}$$

To verify the performance of the Mode division multiplexer, the device was simulated using the COMSOL Multiphysics software based on the finite element method (FEM). According to the light field properties, the calculation domain of the SLNW and LNW is discretized into a nonuniform triangular grid, and the scattering boundary conditions are used to ensure the accuracy of the calculation results.

3. DESIGN OF THE MODE MULTIPLEXER

For the proposed Mode division multiplexer, the pattern properties of the SLNW and LNW are first analyzed to guide the rational choice of structural parameters. The widths of the LNW and SLNW (W_1, W_2) are best selected according to the phase matching conditions, and the TE mode equals the real part of the effective refractive index in the two waveguides. TE0 mode light enters from the In1 port of the LNW waveguide, effectively coupled to the adjacent SLNW by transmitting a certain coupling length and outputs from the crossover port Out2 by mode conversion and coupling to TE1. As can be seen from Fig. 2(a), the TE0 and TE1 modes of the LNW and SLNW increase with the width of the waveguide. The effective refractive index of TE0 at the $W_1 = 450\,\mathrm{nm}$ waveguide is equal to that of TE1 at the $W_2 = 1050\,\mathrm{nm}$ waveguide, or approximately 1.5.

According to the coupling mode theory, the input TE mode enters the optimized coupling region and stimulates the two TE hybrid modes, usually called $\mathrm{TE_{even}}$ and $\mathrm{TE_{odd}}$. The coupling length L_1 is closely associated with the effective refractive index ($n\mathrm{TE_{even}}$ and $n\mathrm{TE_{odd}}$) of the two mixed modes, $\mathrm{TE_{even}}$ and $\mathrm{TE_{odd}}$. As shown in Figs. 3(a)–(b), the effective refractive index of the $\mathrm{TE_{even}}$ and $\mathrm{TE_{odd}}$

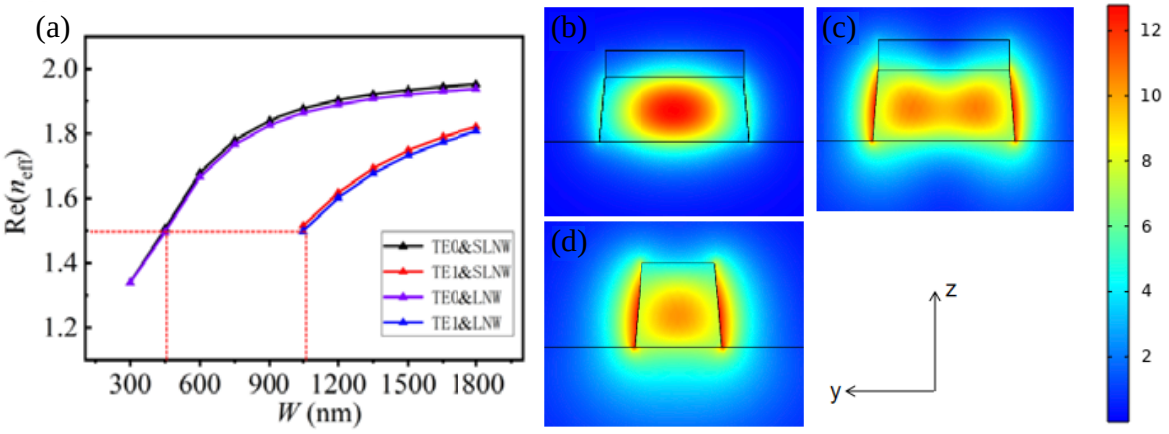

Figure 2. (a) The effective refractive index of the TE0 and TE1 modes in the SLNW and LNW varies with the width, (b) field distribution of TE0 mode in SLNW waveguide, (c) field distribution of TE1 mode in SLNW, and (d) field distribution of TE0 mode in LNW.

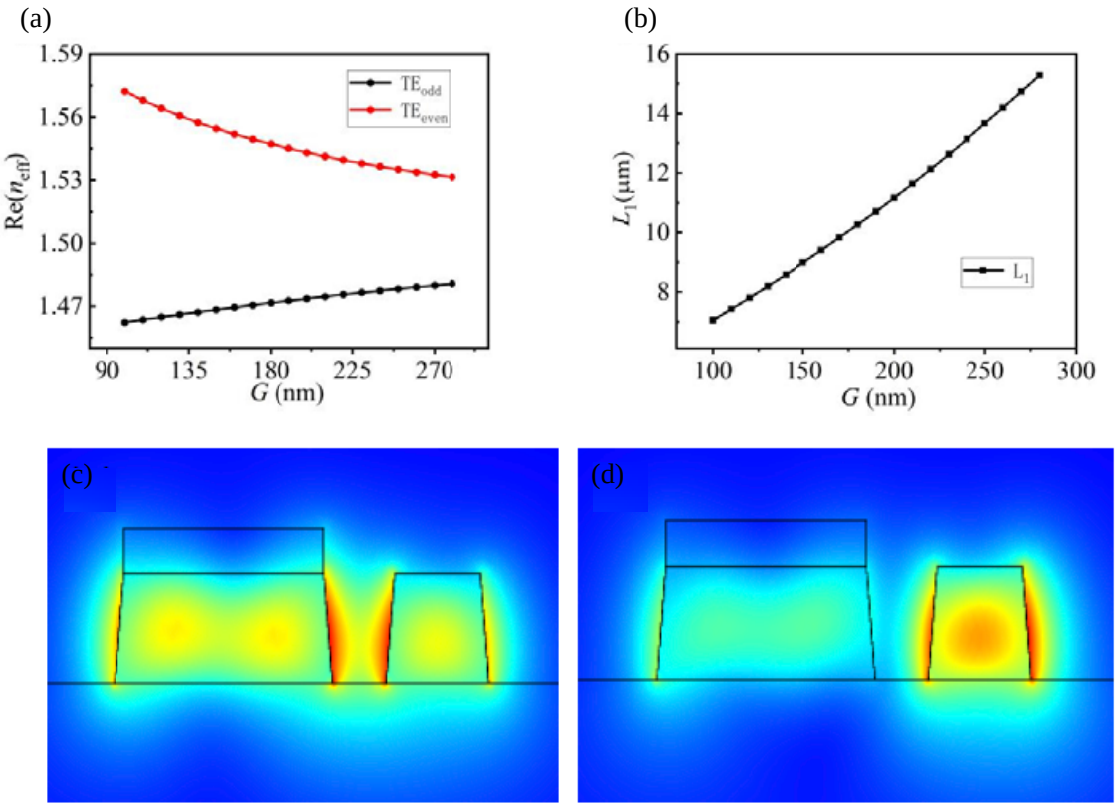

Figure 3. (a) The effective refractive index of the TE_{even} and TE_{odd} modes and (b) the corresponding coupling length L1 and the waveguide spacing G, (c) TE_{even} and (d) TE_{odd}.

modes, the corresponding coupling length L_1, and the spacing between the waveguides G are studied. According to the figure, it can be found that with the increase of the waveguide spacing, the effective refractive index of the TE_{even} mode decreases while the TE_{odd} mode gradually increases, thus increasing the coupling length L_1. However, the waveguide spacing G is closely related to the production process, so it is impossible to decrease infinitely, thus L_1 also has a limit. Here, the waveguide spacing G is chosen as 120 nm, when the calculated coupling length L_1 is 6 μm. It is worth noting that, even when the spacing increases to 280 nm, the coupling length is still less than 16 μm, which is mainly attributed to the strong interaction between the coupled TE modes within the directional coupling region in this device. When $G = 120$ nm, the electric field component distribution diagram of the TE mode in the coupled waveguide, as shown in Figs. 3(c)–(d), designs the size of the two waveguides so that the mode conversion and coupling will occur between the two waveguides. If you inject TE0 mode light into the LNW, it switches to TE1 mode light in the SLNW and is output from the Out2 port. On the other hand, when the TE0 mode light is injected into the SLNW, the mode retains it and is output from the Out2 port.

TE0 mode in LNW and TE1 in SLNW are coupled to form two mixed modes, TE_{even} and TE_{odd}.

$$L_1 = \frac{\lambda}{2\left(n\mathrm{TE}_{even} - n\mathrm{TE}_{odd}\right)} \tag{4}$$

where $n\mathrm{TE}_{even}$ and $n\mathrm{TE}_{odd}$ are the effective refractive indices of TE_{even} and TE_{odd}, and λ is the operating wavelength.

4. CHARACTERISTICS OF MODE DIVISION MULTIPLEXER

To further investigate the properties of the Mode division multiplexer, the geometrical parameter coupling length L_1 and operating wavelength λ are discussed. L_1 and λ are shown in Figs. 4 and 5. At

this point, $W_1 = 450\,\text{nm}$, $W_2 = 1050\,\text{nm}$, $H_1 = 500\,\text{nm}$, and $G = 120\,\text{nm}$.

Figure 4 studies the influence of coupling length L_1 on performance. Fig. 4(a) shows that when TE0 enters port In1, it can be found that the TE0 mode can transmit a specific distance within the coupling region, then be fully coupled to the adjacent SLNW, be transferred forward into the stable TE1 mode in the waveguide, and finally output out of the SLNW outlet Out2. The normalized transmission

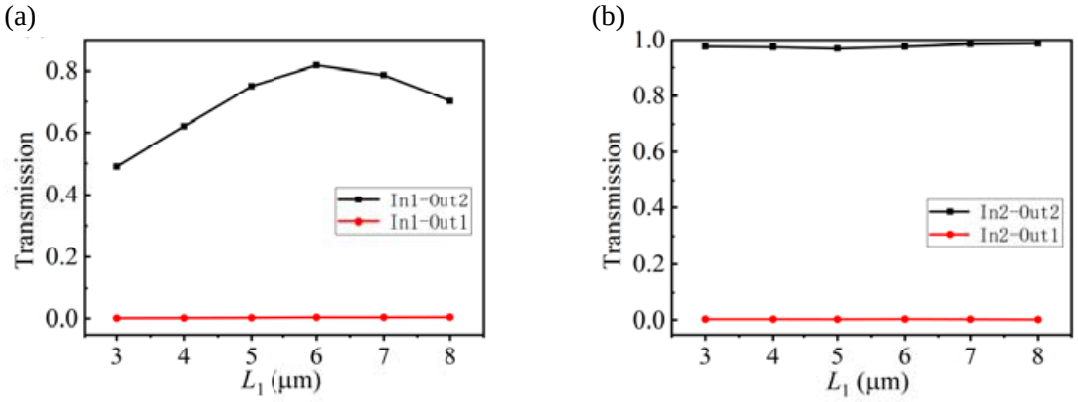

Figure 4. As the coupling length L_1 changes, (a) the effect on normalized transmittance when TE0 enters In1 port and (b) the effect on normalized transmittance when TE0 enters In2 port. Where, $W_1 = 450\,\text{nm}$, $W_2 = 1050\,\text{nm}$, $H_1 = 500\,\text{nm}$, and $G = 120\,\text{nm}$.

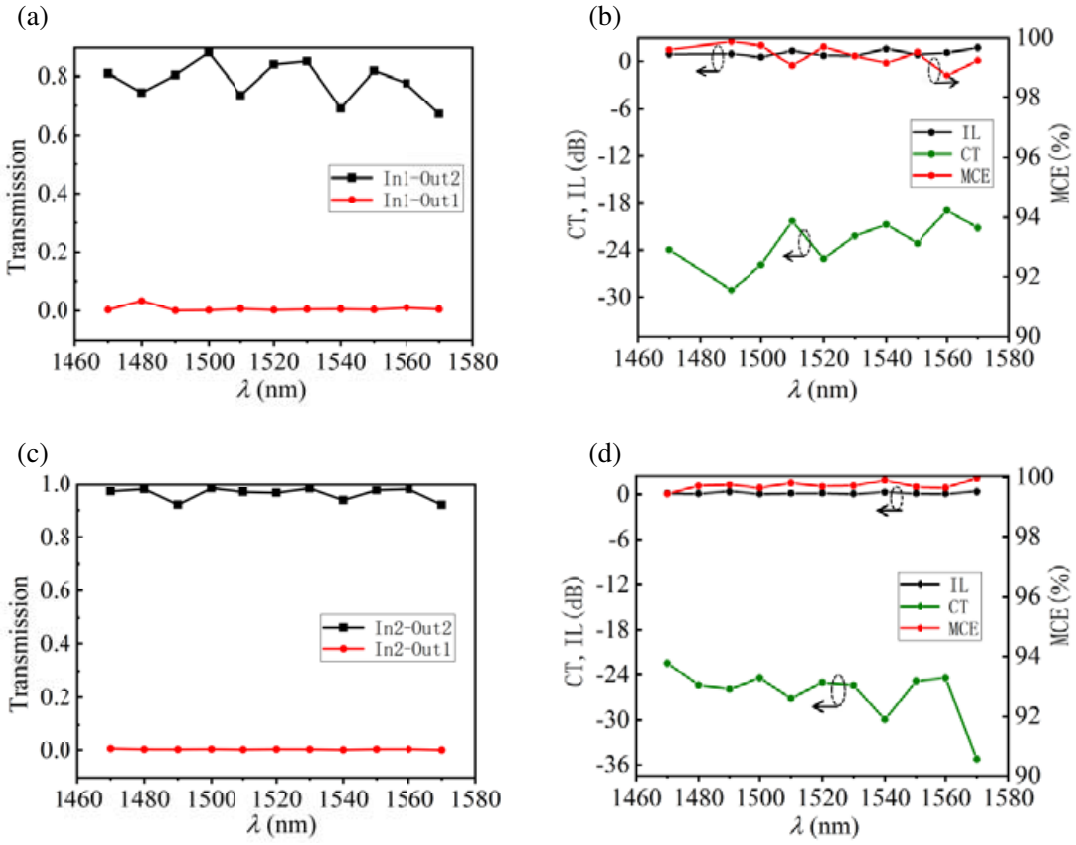

Figure 5. With wavelength λ varying, (a) normalized transmittance and (b) influence of MCE, CT, and IL when TE0 enters In1 port. When TE0 enters the In2 port, (c) normalized transmission (d) effects of MCE, CT, and IL. Where, $W_1 = 450\,\text{nm}$, $W_2 = 1050\,\text{nm}$, $H_1 = 500\,\text{nm}$, and $G = 120\,\text{nm}$.

increases with the increase of L_1 in the range of $3 \sim 6\,\mu m$ and decreases with the increase of L_1 in the range of $6 \sim 8\,\mu m$. When $L_1 = 6\,\mu m$, the normalized transmission reaches the maximum of 0.82. As can be seen from Fig. 4(b), when TE0 enters port In2, it can be found that the normalized transmission power changes little with L_1 and is almost constant. The normalized transmission power of the Out2 port is almost 0, and the normalized transmission power of the Out2 port is almost 1. TE0 comes in through In2 port, is not coupled to the LNW waveguide, and is output directly from the Out2 port. After comprehensive consideration, $L_1 = 6\,\mu m$ is selected.

Figure 5 shows the wavelength dependence of normalized transmittance, IL, CT, and MCE on the TE0 mode input. As can be seen from Fig. 5(a), when TE0 enters In1 port, the normalized transmission power of Out1 port is almost 0. The normalized transmission power at output port 2 is in the form of oscillation, due to the multimode coupling at the output bend. Note that when TE0 enters the In1 port, the TE0 mode is fully coupled to the adjacent SLNW after transmitting a specific distance within the coupling region, and finally output from the SLNW output port Out2. As can be seen from Fig. 5(b), when TE0 enters In1 port, IL is almost 0 dB, MCE value above 98%, and CT value less than -19 dB in wavelength range of $1470 \sim 1570$ nm. As can be seen from Fig. 5(c), when TE0 enters In2 port, the normalized power of Out2 port is almost 1, indicating that TE0 mode is not coupled with SLNW. As shown in Fig. 5(d), in the range of $1470 \sim 1570$ nm, IL was almost 0 dB, MCE value over 99%, and CT value less than -22.5 dB. In general, when $\lambda = 1550$ nm, TE0 enters port In1; the coupling mode is coupled to TE1; and TE1 mode is output from Out2. IL is 0.87 dB, and MCE is 99.5%. When TE0 enters port In2, TE0 mode is output from Out2 with IL of 0.1 dB, MCE of 99.7%, and CT of -25 dB.

After the above discussion, it can be seen that the designed Mode division multiplexer performs the best when $L_1 = 6\,\mu m$ and $\lambda = 1550$ nm. Fig. 6 is a propagation map of light propagation in the waveguide, clearly showing the mode coupling and mode conversion processes in the waveguide. Field distribution (TE-Ey, TE-Ez) in the YZ plane at $W_1 = 450$ nm and $W_2 = 1050$ nm is shown in Fig. 6. As can be seen from Fig. 6(a), when TE0 enters port In2, the TE0 polarized light is not coupled in the coupling region, and it is finally output from the Out2 port. As can be seen from Fig. 6(b), if the TE0 mode is input from the In1 port of the LNW, after mode coupling and mode conversion of TE0 polarized light in the coupling region, TE1 mode exists in the SLNW and is output from Out2 port.

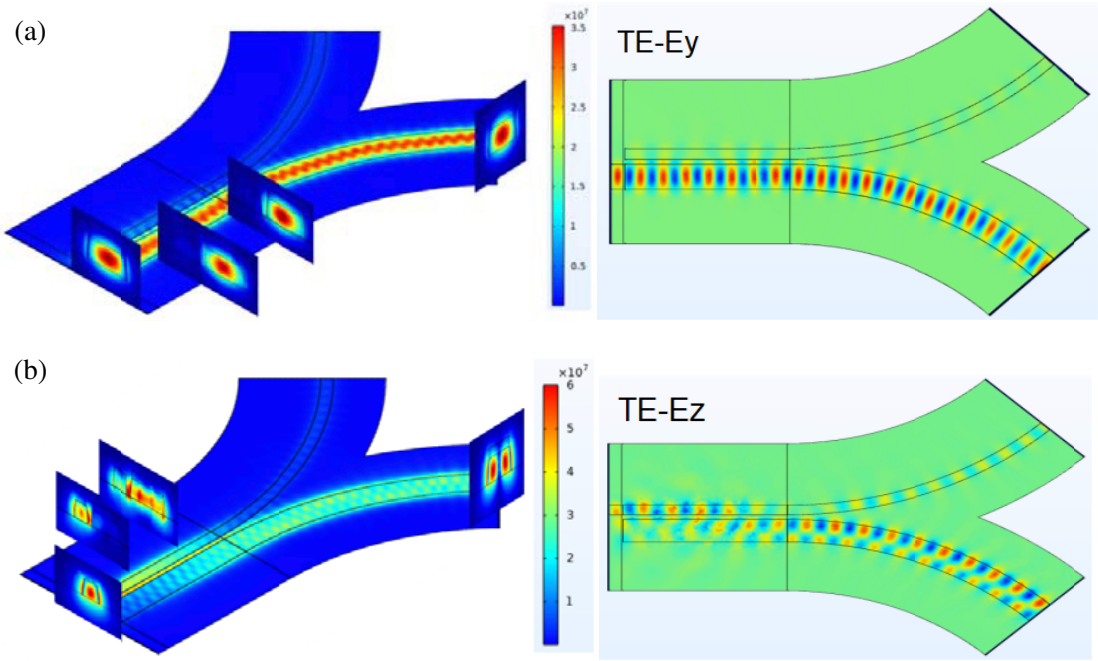

Figure 6. Analog light propagation, (a) TE0 input from In2 port, (b) TE0 input from In1 port. Where, $W_1 = 450$ nm, $W_2 = 1050$ nm, $H_1 = 500$ nm, and $G = 120$ nm.

5. PROPOSED FABRICATION PROCESS

Process design process: The manufacturing process shown in Fig. 7 was used. First, Electron Beam Lithography (EBL) photoresist was deposited on LN thin film. Secondly, Cr was deposited on the top of LN film as a mask etching barrier layer, and the optical waveguide pattern on the mask plate was transferred to the chrome film by EBL exposure development and chemical etching process. The excess LNOI crystal layer was etched, and the remaining metal Cr film was cleaned using an inductively coupled plasma (ICP) process. Finally, SiO_2 at 210 nm thickness was deposited by plasma enhanced chemical vapor deposition (PECVD) [16].

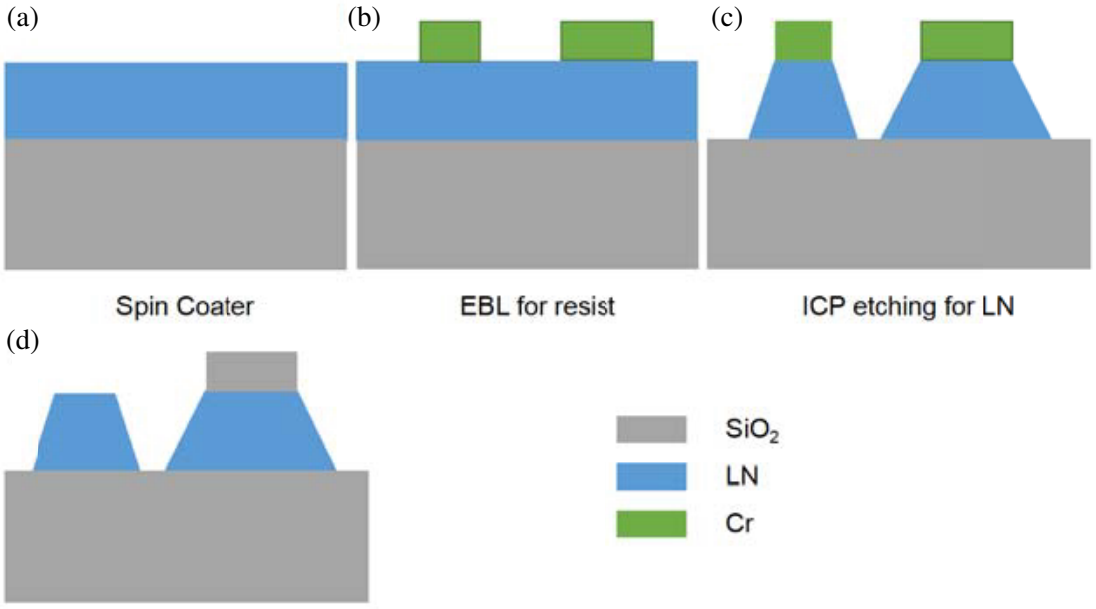

Figure 7. The manufacturing process of modular division multiplexer.

6. CONCLUSION

In summary, an ADC structure ultra-compact mode-division (de)multiplexer with a coupling length of 6 μm is proposed. At the working wavelength of 1.55 μm, when TE0 enters port In1, in the coupling area, the mode is coupled and converted to TE1, and the TE1 mode is output from Out2. The value of IL is 0.87 dB, and the value of MCE is 99.5%. When TE0 enters port In2, the TE0 mode is output from Out2, with 0.1 dB for IL, 99.7% for MCE, and −25 dB for CT. Furthermore, the crosstalk of the on-chip mode multiplexing circuits is less than −19 dB for a 100 nm bandwidth. The device can be extended to more channels, enabling the mode multiplexing system to enhance the ability of TE polarization and can be applied to on-chip optical interconnection and communication.

FUNDING

Natural National Science Foundation of China (NSFC) (62075057).

ACKNOWLEDGMENT

Tao Ma thanks the Key Discipline of Electronic Science and Technology of Henan Province for help identifying collaborators for this work.

REFERENCES

1. Shacham, A., K. Bergman, and L. P. Carloni, "Photonic networks-on-chip for future generations of chip multiprocessors," *IEEE Transactions on Computers*, Vol. 57, No. 9, 1246–1260, 2008.
2. Miller, D., "Device requirements for optical interconnects to silicon chips," *Proceedings of the IEEE*, Vol. 97, No. 7, 1166–1185, 2009.
3. Dai, D., C. Li, S. Wang, et al., "10-channel mode (de)multiplexer with dual polarizations," *Laser & Photonics Reviews*, Vol. 12, No. 1, 2017.
4. Wang, S., X. Feng, S. Guo, et al., "On-chip reconfigurable optical add-drop multiplexer for hybrid wavelength/mode-division-multiplexing systems," *Opt. Lett.*, Vol. 42, No. 14, 2802–2805, Jul. 15, 2017.
5. Dai, D., J. Wang, and Y. Shi, "Silicon mode (de)multiplexer enabling high capacity photonic networks-on-chip with a single-wavelength-carrier light," *Opt. Lett.*, Vol. 38, No. 9, 1422–1424, May 1, 2013.
6. Ding, Y., J. Xu, F. Da Ros, B. Huang, H. Ou, and C. Peucheret, "On-chip two-mode division multiplexing using tapered directional coupler-based mode multiplexer and demultiplexer," *Opt. Express*, Vol. 21, No. 8, 10376–10382, Apr. 22, 2013.
7. Guo, F., D. Liu, R. Zhang, et al., "An MMI-based mode (DE)MUX by varying the waveguide thickness of the phase shifter," *IEEE Photonics Technology Letters*, Vol. 28, No. 21, 2443–2446, 2016.
8. Sun, C., Y. Yu, M. Ye, G. Chen, and X. Zhang, "An ultra-low crosstalk and broadband two-mode (de)multiplexer based on adiabatic couplers," *Sci. Rep.*, Vol. 6, 38494, Dec. 6, 2016.
9. Wu, Y. and K. S. Chiang, "Ultra-broadband mode multiplexers based on three-dimensional asymmetric waveguide branches," *Opt. Lett.*, Vol. 42, No. 3, 407–410, Feb. 1, 2017.
10. Yang, Y. D., Y. Li, Y. Z. Huang, and A. W. Poon, "Silicon nitride three-mode division multiplexing and wavelength-division multiplexing using asymmetrical directional couplers and microring resonators," *Opt. Express*, Vol. 22, No. 18, 22172–22183, Sep. 8, 2014.
11. Xing, J., Z. Li, X. Xiao, J. Yu, and Y. Yu, "Two-mode multiplexer and demultiplexer based on adiabatic couplers," *Opt. Lett.*, Vol. 38, No. 17, 3468–3470, Sep. 1, 2013.
12. Uematsu, T., Y. Ishizaka, Y. Kawaguchi, K. Saitoh, and M. Koshiba, "Design of a compact two-mode multi/demultiplexer consisting of multimode interference waveguides and a wavelength-insensitive phase shifter for mode-division multiplexing transmission," *Journal of Lightwave Technology*, Vol. 30, No. 15, 2421–2426, 2012.
13. Chen, W., P. Wang, T. Yang, et al., "Silicon three-mode (de)multiplexer based on cascaded asymmetric Y junctions," *Opt. Lett.*, Vol. 41, No. 12, 2851–2854, Jun. 15, 2016.
14. Sun, Y., Y. Xiong, and W. N. Ye, "Experimental demonstration of a two-mode (de)multiplexer based on a taper-etched directional coupler," *Opt. Lett.*, Vol. 41, No. 16, 3743–3746, Aug. 15, 2016.
15. Hu, H., R. Ricken, and W. Sohler, "Lithium niobate photonic wires," *Opt. Express*, Vol. 17, 24261–24268, 2009.
16. Cheng, Z. J. Wang, Y. Huang, and X. Ren, "Realization of a compact broadband polarization beam splitter using the three-waveguide coupler," *IEEE Photonics Technology Letters*, Vol. 31, 3, 2019.